

Quench dynamics and defects formation in the Ising chain in a transverse magnetic field

Alexander I Nesterov*

*Departamento de Física, CUCEI, Universidad de Guadalajara,
Av. Revolución 1500, Guadalajara, CP 44420, Jalisco, México*

Mónica F Ramírez†

Tepatitáns Institute for Theoretical Studies, Tepatitán, Jalisco, México

(Dated: February 6, 2022)

We study analytically and numerically quench dynamics and defects formation in the quantum Ising model in the presence of a time-dependent transverse magnetic field. We generalize the Landau-Zener formula to the case of non-adiabatic evolution of the quantum system. For a quasi-static magnetic field, with a slow dependence on time, our outcomes are similar to the results predicted by the Landau-Zener formula. However, a quench dynamics under a shock-wave load is more complicated. The final state of the system depends on the amplitude and pulse velocity, resulting in the mixture of ground and excited states and significant density of defects.

PACS numbers: 75.30.Wx, 03.65.-w, 03.65.Vf

Keywords: Energy-level crossing Ising chain quantum phase transition quench dynamics

I. INTRODUCTION

Quantum phase transitions (QPTs) are characterized by qualitative changes of the ground state of many body system and occur at the zero temperature [1]. Since thermal fluctuations are frozen, QPTs are purely quantum phenomena driven by quantum fluctuations. Well known examples of QPTs are the superconductor to insulator transition in high- T_c superconducting systems, the quantum paramagnet to ferromagnet transition occurring in Ising spin system under an external transverse magnetic field, and the superfluid to Mott insulator transition.

QPTs are associated with levels crossing and imply the lost analyticity in the energy spectrum. In the parameter space the points of non-analyticity, being referred to as critical points, define the QPT [1]. A first-order QPT is determined by a discontinuity in the first derivative of the ground state energy. A second-order QPT means that the first derivative is continuous, while the second derivative has either a finite discontinuity or divergence at the critical point.

Energy level crossing implies that it does not matter how slowly the system is evolved. Near the critical point adiabaticity breaks down and non-equilibrium phenomena associated with

the drastically grown quantum fluctuations can drive the system away from the ground state. The final result depends on how fast the transition occurs. If the quench process is sufficiently fast, large numbers of topological defects are created and the final state can be essentially different from that been obtained as result of slow evolution. Qualitatively, the dynamics of quantum system can be described by the Kibble-Zurek (KZ) theory of nonequilibrium phase transitions [2–4].

In this paper we consider quench dynamics of the quantum of Ising chain in a transverse time-dependent magnetic field. The paper is organized as follows: In Sec. II we introduce the model and discuss its main features. In Sec. III we study quench dynamics for a magnetic field defined by a pulse of a given shape. In Sec. IV we describe defects formation near of critical point. We conclude in Sec. V with a discussion of our results.

II. DESCRIPTION OF THE MODEL

We consider the one-dimensional Ising model in a transverse magnetic field governed by the following Hamiltonian:

$$\mathcal{H} = -\frac{J}{2} \sum_{n=1}^N (h\sigma_n^x + \sigma_n^z \sigma_{n+1}^z), \quad (1)$$

where the periodic boundary conditions, $\sigma_{N+1} = \sigma_1$, are imposed. The external magnetic field is associated with the parameter h .

*Electronic address: nesterov@cencar.udg.mx

†Electronic address: monica.felipa@gmail.com

Quantum phase transition (QPT) occurs in the thermodynamic limit ($N \gg 1$) at critical value $h_c = 1$ of the external magnetic field.

The Hamiltonian in Eq. (1) can be diagonalized using the standard Jordan-Wigner transformation, following well-known procedures described in [5–9]. The Jordan-Wigner transformation maps a spin-1/2 system to a system of spinless fermions,

$$\sigma_n^x = 1 - 2c_n^\dagger c_n, \quad (2)$$

$$\sigma_n^y = i(c_n^\dagger - c_n) \prod_{m < n} (1 - 2c_m^\dagger c_m), \quad (3)$$

$$\sigma_n^z = -(c_n + c_n^\dagger) \prod_{m < n} (1 - 2c_m^\dagger c_m), \quad (4)$$

with anticommutation relations: $\{c_m^\dagger, c_n\} = \delta_{mn}$ and $\{c_m, c_n\} = \{c_m^\dagger, c_n^\dagger\} = 0$. Applying these transformations, we obtain

$$\mathcal{H} = -\frac{J}{2} \sum_{n=1}^N (c_n^\dagger c_{n+1} + c_{n+1}^\dagger c_n + c_n^\dagger c_{n+1}^\dagger + c_{n+1} c_n + h(1 - 2c_n^\dagger c_n)). \quad (5)$$

The periodic boundary conditions imposed on the spin operators lead to the following condition for the fermionic operators:

$$c_{N+1} = -e^{i\pi\mathcal{N}_F} c_1, \quad (6)$$

$\mathcal{N}_F = \sum_{n=1}^N c_n^\dagger c_n$ being the total number of fermions. Using Eq. (2) we find that $\mathcal{N}_F = N/2 - S^x$, where $S^x = (1/2) \sum_n \sigma_n^x$ is the total x -component of the spins. For the particular choice of $S^x = 0$, we obtain $\mathcal{N}_F = N/2$. This yields periodic *periodic* (*antiperiodic*) boundary

conditions for c_n , if $N/2$ is *odd* (*even*). Since the parity of the fermions is conserved, the imposed boundary conditions are valid for all values of the parameter h .

Applying the Fourier transformations,

$$c_n = \frac{e^{-i\pi/4}}{\sqrt{N}} \sum_k c_k e^{i2\pi kn/N}, \quad (7)$$

we find that the Hamiltonian (5) can be recast in Fourier space as

$$\mathcal{H} = \frac{J}{2} \sum_k \left(2(h - \cos \varphi_k) c_k^\dagger c_k - h + \sin \varphi_k (c_k^\dagger c_{-k}^\dagger + c_{-k} c_k) \right), \quad (8)$$

where $\varphi_k = 2\pi k/N$. For periodic boundary conditions, $c_{N+1} = c_1$, the wave number k takes the following discrete values:

$$k = -\frac{N}{2}, \dots, 0, 1, \dots, \frac{N}{2} - 1, \quad (9)$$

and for antiperiodic boundary conditions, $c_{N+1} = -c_1$, one has

$$k = \pm \frac{1}{2}, \pm \frac{3}{2}, \dots, \pm \frac{N-1}{2}. \quad (10)$$

Here we set lattice spacing $a = 1$. In what follows, we impose the antiperiodic boundary conditions for the fermionic operators.

The Hamiltonian (8) can be diagonalized by

using the Bogoliubov transformation,

$$c_k = \cos \frac{\theta_k}{2} a_k + \sin \frac{\theta_k}{2} a_{-k}^\dagger, \quad (11)$$

$$c_k^\dagger = \cos \frac{\theta_k}{2} a_k^\dagger + \sin \frac{\theta_k}{2} a_{-k}, \quad (12)$$

$$a_k = \cos \frac{\theta_k}{2} c_k + \sin \frac{\theta_k}{2} c_{-k}^\dagger, \quad (13)$$

$$a_k^\dagger = \cos \frac{\theta_k}{2} c_k^\dagger + \sin \frac{\theta_k}{2} c_{-k}, \quad (14)$$

where

$$\cos \theta_k = \frac{h - \cos \varphi_k}{\sqrt{h^2 - 2h \cos \varphi_k + 1}}, \quad (15)$$

$$\sin \theta_k = \frac{\sin \varphi_k}{\sqrt{h^2 - 2h \cos \varphi_k + 1}}. \quad (16)$$

With help of Eqs. (11) – (14) we obtain the diagonalized Hamiltonian as a sum of quasiparticles with half-integer quasimomenta,

$$\mathcal{H} = \frac{1}{2} \sum_k \varepsilon_{0k} + \sum_k \varepsilon_k \left(a_k^\dagger a_k + \frac{1}{2} \right). \quad (17)$$

where $\varepsilon_{0k} = J(h - \cos \varphi_k)$ and

$$\varepsilon_k = J\sqrt{h^2 - 2h \cos \varphi_k + 1}. \quad (18)$$

Its spectrum contains only states with even number of quasiparticles.

In the momentum representation, the Hamiltonian splits into a sum of independent terms, $\mathcal{H} = \sum_{k>0} \mathcal{H}_k$, where each \mathcal{H}_k acts in the two-dimensional Hilbert space spanned by $|k_0\rangle = |0\rangle_k |0\rangle_{-k}$ and $|k_1\rangle = |1\rangle_k |1\rangle_{-k}$. Here $|0\rangle_k$ is the vacuum state of the mode c_k , and $|1\rangle_k$ is the excited state: $|1\rangle_k = c_k^\dagger |0\rangle_k$. The total wavefunction can be written as, $|\psi(t)\rangle = \bigotimes_{k>0} |\psi_k(t)\rangle$, where

$$|\psi_k(t)\rangle = u_k(t)|k_0\rangle + v_k(t)|k_1\rangle, \quad (19)$$

and $|\psi_k\rangle$ satisfies the Bogoliubov-de Gennes equation (in units $\hbar = 1$):

$$i \frac{\partial}{\partial t} |\psi_k\rangle = \mathcal{H}_k(t) |\psi_k\rangle. \quad (20)$$

Choosing the basis as, $k_1 = \begin{pmatrix} 1 \\ 0 \end{pmatrix}$ and $k_0 = \begin{pmatrix} 0 \\ 1 \end{pmatrix}$, one can show that the Hamiltonian, \mathcal{H}_k , projected on this two-dimensional subspace takes the form,

$$\mathcal{H}_k = \varepsilon_{0k} \mathbb{1} + J \begin{pmatrix} h - \cos \varphi_k & \sin \varphi_k \\ \sin \varphi_k & -h + \cos \varphi_k \end{pmatrix}. \quad (21)$$

For each k , there are two eigenstates:

$$|u_+(k)\rangle = \begin{pmatrix} \cos \frac{\theta_k}{2} \\ \sin \frac{\theta_k}{2} \end{pmatrix}, \quad (22)$$

$$|u_-(k)\rangle = \begin{pmatrix} -\sin \frac{\theta_k}{2} \\ \cos \frac{\theta_k}{2} \end{pmatrix}. \quad (23)$$

Since $\mathcal{H} = \sum_{k>0} \mathcal{H}_k$, the ground state of the Ising chain can be written as a product of qubit-like states:

$$|\psi_g\rangle = \bigotimes_{k>0} \left(\cos \frac{\theta_k}{2} |0\rangle_k |0\rangle_{-k} - \sin \frac{\theta_k}{2} |1\rangle_k |1\rangle_{-k} \right). \quad (24)$$

For $h \gg 1$, the ground state is paramagnetic with all spins oriented along the x axis, and from Eq. (15) we obtain $\cos \theta_k \rightarrow 1$ as $h \rightarrow \infty$. This yields $|u_-(k)\rangle \rightarrow \begin{pmatrix} 0 \\ 1 \end{pmatrix}$ and $|u_+(k)\rangle \rightarrow \begin{pmatrix} 1 \\ 0 \end{pmatrix}$. On the other hand, when $h \ll 1$ there are two degenerate ferromagnetic ground states with all spins polarized in opposite directions along the z -axis. In the thermodynamic limit the system passing through the critical point ends in a superposition of up and down states with finite domains of spins separated by kinks [10].

III. QUENCH DYNAMICS

A. Adiabatic and non-adiabatic evolution

We consider quantum Ising chain driven by time-dependent Hamiltonian, $\mathcal{H}(t) = \sum_k \mathcal{H}_k(t)$, where

$$\mathcal{H}_k(t) = \varepsilon_{0k}(t) \mathbb{1} + J \begin{pmatrix} h(t) - \cos \varphi_k & \sin \varphi_k \\ \sin \varphi_k & -h(t) + \cos \varphi_k \end{pmatrix}. \quad (25)$$

For a generic quantum system governed by

the time-dependent Hamiltonian the adiabatic

theorem guarantees that during quantum evolution the system remains in its the ground state, as long as the instantaneous ground state does not become degenerate at any time. The validity of the adiabatic theorem requires

$$\sum_{m \neq n} \left| \frac{\langle \psi_m | \partial \mathcal{H}(t) / \partial t | \psi_n \rangle}{(E_m - E_n)^2} \right| \ll 1. \quad (26)$$

When the quantum processes is related to the quantum phase transitions, the condition of Eq. (26) can be recast as [14, 15],

$$\frac{|\langle \psi_e | \partial \mathcal{H}(t) / \partial t | \psi_g \rangle|}{|E_e - E_g|^2} \ll 1, \quad (27)$$

where $|\psi_g\rangle$ is the ground state, and E_e is the energy of the first excited state, $|\psi_e\rangle$. This restriction is violated near the degeneracy in which the QPT occurs.

In the adiabatic basis formed by the instantaneous eigenvectors of the Hamiltonian H_k , the total wavefunction can be written, as $|\psi\rangle = \otimes_k |\psi_k(t)\rangle$, where

$$|\psi_k(t)\rangle = \alpha_k(t) e^{i \int \varepsilon_{0k}(t) dt} |u_-(k, t)\rangle + \beta_k(t) e^{i \int \varepsilon_{0k}(t) dt} |u_+(k, t)\rangle. \quad (28)$$

From Eqs. (22) and (23) it follows that

$$\alpha_k(t) = u_k(t) \cos \frac{\theta_k(t)}{2} - v_k(t) \sin \frac{\theta_k(t)}{2}, \quad (29)$$

$$\beta_k(t) = v_k(t) \cos \frac{\theta_k(t)}{2} + u_k(t) \sin \frac{\theta_k(t)}{2}. \quad (30)$$

We define

$$|\Psi_k(t)\rangle = \begin{pmatrix} \beta_k(t) \\ \alpha_k(t) \end{pmatrix}. \quad (31)$$

Next, one can show that the wave function, $|\Psi_k(t)\rangle$, satisfies the Bogoliubov-de Gennes equation

$$i \frac{\partial}{\partial t} |\Psi_k\rangle = H_k(t) |\Psi_k\rangle, \quad (32)$$

where

$$H_k = \varepsilon_{0k} \mathbb{1} + \begin{pmatrix} \varepsilon_k & i\dot{\theta}_k/2 \\ -i\dot{\theta}_k/2 & -\varepsilon_k \end{pmatrix}, \quad (33)$$

and

$$\frac{d\theta_k}{dt} = - \frac{\dot{h}(t) \sin^2 \theta_k(t)}{\sin \varphi_k} \quad (34)$$

Now the requirement of the adiabatic theorem (27) can be rewritten as,

$$\max \left| \frac{d\theta_k}{dt} \right| \ll \min 2\varepsilon_k = 2J \sin \varphi_k. \quad (35)$$

Employing (35), one can recast Eq. (34) as,

$$|\dot{h}_c| \ll 2J \sin^2 \varphi_k, \quad (36)$$

where $\dot{h}_c = \dot{h}(t_c)$. Here t_c denotes the moment of time when the magnetic field reached its critical value, $h_c = 1$. Further, it is convenient to introduce the following notation:

$$\omega_k^2 = \frac{J \sin^2 \varphi_k}{|\dot{h}_c|}. \quad (37)$$

Using (37) in Eq. (36), we find that for the given value of k the condition of adiabaticity can be written as $\omega_k^2 \gg 1$. As follows from Eq. (27), for the whole system the condition of adiabaticity can be written as, $\omega^2 \gg 1$, where

$$\omega^2 \equiv \omega_1 = \frac{J}{|\dot{h}_c|} \sin^2 \left(\frac{\pi}{N} \right) \gg 1. \quad (38)$$

For $N \gg 1$ we obtain

$$\omega^2 = \frac{\pi^2 J}{|\dot{h}_c| N^2} \gg 1. \quad (39)$$

Let us assume that the dependence of the magnetic field on time has the form $h = h(t/\tau_0)$. By presenting,

$$\alpha_k(t) = a_k(t) e^{i \int_0^t \varepsilon(k,t) dt}, \quad (40)$$

$$\beta_k(t) = b_k(t) e^{-i \int_0^t \varepsilon(k,t) dt}, \quad (41)$$

one can show that, if the evolution begins from the ground state, the coefficients $a_k(t)$ and $b_k(t)$ satisfy the following asymptotic conditions [16–24]:

$$b_k(t) = \mathcal{O} \left(\exp \left(2\tau_0 \int_0^{z_c} \varepsilon_k(z) dz \right) \right), \quad (42)$$

where the critical point, z_c , lies on the first Stokes line in the *lower* complex line defined as

$$\Im \int_0^{z_c} \varepsilon_k(z) dz < 0. \quad (43)$$

The critical point is determined as a solution of the equation, $\varepsilon_k(z_c) = 0$, in the complex plane obtained by analytical continuation, $t \rightarrow z$.

Employing (18), we find that for the Ising model the integral in the r.h.s. of Eq. (42) can be recast as follows:

$$\int_0^{z_c} \varepsilon_k(z) dz = \int_0^{e^{-i\varphi_k}} \sqrt{Z^2 - 2Z \cos \varphi_k + 1} \frac{dZ}{Z'}, \quad (44)$$

where $Z' = dZ/dz$, and we set $Z = h(z)$.

For given k , the probability to stay in the ground state at the end of the evolution is given by $P_k^{gs}(t) = |\alpha_k(t)|^2$. With help of Eq. (42) we obtain

$$P_k^{gs}(\infty) = 1 - |\beta_k(t)|^2 \approx 1 - e^{4\tau_0 \Im \int_0^{z_c} \varepsilon_k(z) dz} \quad (45)$$

Since different pairs of quasiparticles ($k, -k$) evolve independently, the probability to stay in the ground state for the whole system is the product [10]

$$P_{gs} = \prod_{k>0} P_{gs}(k). \quad (46)$$

For slow evolution one can use the LZ approximation in Eq. (44), that consists in changing $Z'(z)$ by its value in the critical point, $Z'(z_c)$. Performing integration in (44) and inserting the result in (45), we obtain the Landau Zener formula [25, 26]

$$P_k^{gs} \approx 1 - e^{-\pi\omega_k^2}, \quad (47)$$

where $\omega_k^2 = (J/|\dot{h}_c|)\sin^2 \varphi_k$. This result is valid when $\omega_k^2 \gg 1$, that is in agreement with the condition (38). By applying (46) we find that the probability to stay in the ground state for the whole system is

$$P_{gs} = \prod_{k>0} (1 - e^{-\pi\omega_k^2}). \quad (48)$$

B. Adiabatic-impulse approximation

In according to KZ mechanism, the main contribution to the QPT is made in the neighborhood of the critical point [2–4]. Expanding $h(t)$ near of critical point as $h(t) = 1 + \dot{h}_c(t - t_c)$, one can rewrite (25) as follows (we omit unessential diagonal contribution, ε_{0k}),

$$\mathcal{H}_k(t) \approx J \begin{pmatrix} \dot{h}_c(t - t_c) + 2 \sin^2(\varphi_k/2) & \sin \varphi_k \\ \sin \varphi_k & -\dot{h}_c(t - t_c) - 2 \sin^2(\varphi_k/2) \end{pmatrix}. \quad (49)$$

It convenient to introduce a new variable, $\tau_k = (J/\kappa)(t - t_c) + \text{sgn}(\dot{h}_c)2\kappa \sin^2(\varphi_k/2)$, where $\kappa = \sqrt{J/|\dot{h}_c|}$. Let us assume that $\dot{h}_c < 0$, then the Hamiltonian (25) takes the form of the LZ model,

$$\hat{\mathcal{H}}_k = \begin{pmatrix} -\tau_k & \omega_k \\ \omega_k & \tau_k \end{pmatrix}, \quad (50)$$

the coupling strength being $\omega_k = \kappa \sin \varphi_k$. Qualitatively, the dynamics of the LZ system can be described by using so-called the *adiabatic-impulse* (AI) approximation [11–13]. The AI-approximation assumes that the whole evolution can be divided in three parts, and up to the phase factor the wave function, $|\psi_k(t)\rangle$, approximately can be described as

$$\begin{aligned} \tau_k \in [-\infty, -\hat{\tau}_k) : & \quad |\psi_k(\tau_k)\rangle \approx |u_-(k, \tau_k)\rangle \\ \tau_k \in [-\hat{\tau}_k, \hat{\tau}_k) : & \quad |\psi_k(\tau_k)\rangle \approx |u_-(k, -\hat{\tau}_k)\rangle \\ \tau_k \in (\hat{\tau}_k, +\infty) : & \quad |\langle \psi_k(\tau_k) | u_-(k, \tau) \rangle|^2 = \text{const} \end{aligned}$$

where the time $\hat{\tau}_k$, introduced by Zurek [3], is called the *freeze-out time* and define the instant when behaviour of the system changes from the adiabatic regime to an impulse one where its state is effectively frozen and then back from the impulse regime to the adiabatic one.

If the evolution starts at moment $\tau_i \ll -\hat{\tau}_k$ from the ground state, the equation for determining $\hat{\tau}_k$ can be written as $\pi \hat{\tau}_k = 1/\varepsilon_k(\hat{\tau}_k)$ (for details of calculation, see reference [11]). Its solution is given by

$$\hat{\tau}_k = \frac{\omega_k}{\sqrt{2}} \sqrt{\sqrt{1 + \frac{4}{\pi^2 \omega_k^4}} - 1}. \quad (51)$$

In the AI approximation the probability, P_{ex}^k , of exciting mode k at $\tau_f \gg \hat{\tau}_k$ can be calculated as follows [11, 13]:

$$P_{ex}^k \approx P_{AI}^k = |\langle u_+(k, \hat{\tau}_k) | u_-(k, -\hat{\tau}_k) \rangle|^2 = \frac{\hat{\tau}_k^2}{\omega_k^2 + \hat{\tau}_k^2}. \quad (52)$$

Substituting $\hat{\tau}_k$ from (51), we obtain

$$P_{ex}^k = \frac{2}{x_k^2 + x_k \sqrt{x_k^2 + 4} + 2}, \quad (53)$$

where $x_k = \pi\omega_k^2$. For $\omega_k^2 \ll 1$, from Eq. (53) it follows $P_{AI}^k \approx 1 - \pi\omega_k^2$. In the first order this coincides with the result predicted by exact LZ formula: $P_{ex}^k = e^{-\pi\omega_k^2}$. For the adiabatic evolution, $\omega_k^2 \gg 1$, we obtain $P_{AI}^k \approx 1/(\pi^2\omega_k^4)$.

Employing (46) we find that in the AI-approximation the probability to stay in the ground state for the whole system is given by

$$P_{gs} = \prod_{k>0} \frac{x_k^2 + x_k \sqrt{x_k^2 + 4}}{x_k^2 + x_k \sqrt{x_k^2 + 4} + 2}. \quad (54)$$

In the thermodynamic limit, the variable φ_k becomes continuous, and we obtain

$$P_{ex}(\kappa, \varphi) = \frac{2}{x^2 + x \sqrt{x^2 + 4} + 2}, \quad (55)$$

where $x = \pi\kappa^2 \sin^2 \varphi$. In Fig. 1 the probability of finding the system in excited state is presented. One can see that for $\kappa \gg 1$ the main contribution to $P_{ex}(\kappa, \varphi)$ is occurred from the values of $\varphi \approx 0$ and $\varphi \approx \pi$. In other limit, $\kappa \ll 1$, the values of $\varphi \approx \pi/2$ yield the most important contribution to the probability $P_{ex}(\kappa, \varphi)$.

IV. QUENCH DYNAMICS UNDER SHOCK-WAVE LOAD

A. Semi-finite pulse

1. Transition from paramagnet to ferromagnet

During its evolution the system does not remain in the ground state at all times. At the critical point, the quantum system becomes excited, and its final state is determined by the number of defects. In the case of the ferromagnetic Ising chain and for transition: *paramagnet* \rightarrow *ferromagnet*, the system ends in the state such as

$$| \dots \uparrow\uparrow\uparrow\uparrow\downarrow\downarrow\downarrow\downarrow \dots \downarrow\downarrow\uparrow\uparrow\uparrow \dots \uparrow\uparrow\downarrow\downarrow \dots \rangle$$

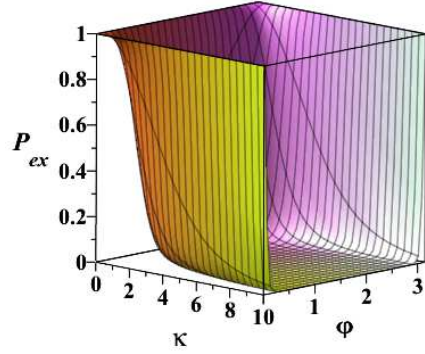


FIG. 1: (Color online) Probability of finding the system in the excited state as a function of $\kappa = \sqrt{J/|\hbar_c|}$ and φ .

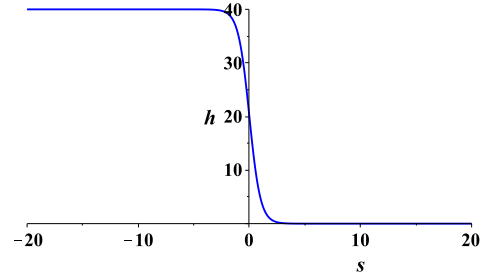


FIG. 2: (Color online) Shape of semi-finite pulse: h vs $s = t/\tau_0$ ($h_0 = 20$).

with neighboring spins polarized in the same directions along the z -axis and separated by kinks (defects) in which the polarization of spins has the opposite orientation.

We specify the magnetic field as a semi-finite pulse with the shape determined by (Fig. 2)

$$h = h_0(1 - \tanh(t/\tau_0)). \quad (56)$$

The height of the pulse is given by $h_m = 2h_0$. At the critical point, $h_c = 1$, we have

$$\dot{h}_c = -\frac{2}{\tau_0} \left(1 - \frac{1}{2h_0}\right). \quad (57)$$

It turns out convenient to introduce a dimensionless time $s = t/\tau_0$ and to recast the Bogoliubov-de Gennes equation (32) as,

$$i \frac{\partial}{\partial s} |\Psi_k(s)\rangle = \hat{H}_k(s) |\Psi_k(s)\rangle, \quad (58)$$

where

$$\hat{H}_k = \hat{\varepsilon}_{0k} \mathbb{1} + \begin{pmatrix} \hat{\varepsilon}_k & i\theta'_k/2 \\ -i\theta'_k/2 & -\hat{\varepsilon}_k \end{pmatrix}. \quad (59)$$

We set $\theta'_k = d\theta_k/ds$, $\hat{\varepsilon}_{0k} = \tau_0 \varepsilon_{0k}$, and $\hat{\varepsilon}_k =$

$\tau_0 \varepsilon_k$.

To estimate asymptotic behavior of the probability to stay in the ground state we use Eq. (45). The result is

$$P_{gs} = \prod_k (1 - e^{-4\tau_0 \Im \int_0^{z_c} \varepsilon_k(z) dz}) \quad (60)$$

Using (56) in Eq. (44), we are performing integration to obtain

$$4\Im \int_0^{z_c} \varepsilon_k(z) dz = \pi J \tau_0 (\sqrt{h_m^2 - 2h_m \cos \varphi + 1} + 1 - h_m) \quad (61)$$

Then the probability to stay in the ground state at the end of evolution can be written as

$$P_{gs} = \prod_{k>0} (1 - e^{-\pi \nu_k^2}), \quad (62)$$

where

$$\nu_k^2 = \tau_0 J (\sqrt{h_m^2 - 2h_m \cos \varphi + 1} + 1 - h_m). \quad (63)$$

For $h_m \gg 1$ this yields

$$\nu_k^2 \approx 2J\tau_0 \sin^2 \frac{\varphi_k}{2}. \quad (64)$$

Since ω_k does not includes h_m , in the end of evolution the state of system is insensitive to changing of amplitude. Computation of the parameter of adiabaticity, ω_k , yields

$$\omega_k^2 = \frac{J\tau_0 \sin^2 \varphi_k}{2}. \quad (65)$$

For long wavelength modes with $\varphi_k \ll \pi/4$ we obtain $\nu_k \approx \omega_k$.

Our theoretical predictions are confirmed by numerical calculations performed for $N = 32, 48, 64, 128, 256, 512$ spins (See Figs. 3, 4.). We assume that initially the system was in the ground (paramagnet) state. Choice of parameters: $J = 1$, $\tau_0 = 500$, $h_0 = 20$. Solid lines present the results of the numerical simulations and dashed lines correspond to the asymptotic formula (62). One can observe that while short wavelength excitations are essential at the critical point, at the end of evolution their contribution to the transition probability from the

ground state to the first excited state is negligible. The results presented in Fig. 3a show that the asymptotic formula (62) is in good agreement with the results of numerical simulations.

The estimation of the adiabaticity parameter ω (see Eq.(38)) yields: $\omega = 2.4$ ($N = 32$), $\omega = 1.07$ ($N = 48$), $\omega = 0.6$ ($N = 64$), $\omega = 0.15$ ($N = 128$), $\omega = 0.04$ ($N = 256$), $\omega = 0.01$ ($N = 512$). As expected, with decreasing of ω the probability to stay in the ground state decreases as well. This implies that at the end of evolution the quantum system does not remains in the ground state and its final state is the superposition of blocks with the spins oriented up/down, separated by walls (kinks).

2. Transition from ferromagnet to paramagnet

To describe transition from ferromagnet to paramagnet, we specify the magnetic field as a semi-infinite pulse with the shape determined by (See Fig. 5.)

$$h = h_0 (1 + \tanh(t/\tau)), \quad (66)$$

height of the pulse being $h_m = 2h_0$.

We start with the initial ferromagnet ground state. Near the critical point, the quantum system becomes excited, and its final state (for $h_0 \gg 1$) is determined by the number of flipped spins.

We find that asymptotic behavior of the probability to stay in the ground state is given by

$$P_{gs}(\infty) = \prod_k (1 - e^{-\pi \nu_k^2}), \quad (67)$$

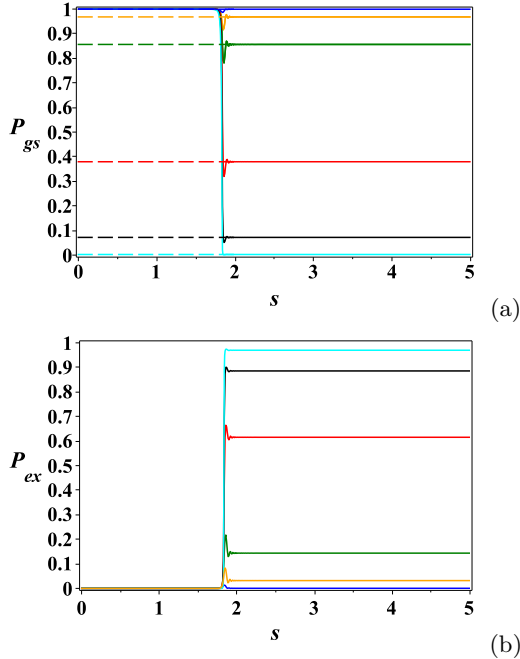


FIG. 3: (Color online) (a) The probability, P_{gs} , to stay in the ground state as a function of the dimensionless time $s = t/\tau$. (b) The probability P_{ex} of first excited state ($k = 1$) vs s . Parameters used: $\tau = 500$, $h_0 = 20$. Blue line ($N = 32$), orange line ($N = 48$), green line ($N = 64$), red line ($N = 128$), black line ($N = 256$), cyan line ($N = 512$). Dashed lines correspond to the asymptotic formula (62).

where

$$\nu_k^2 = J\tau_0(\sqrt{h_m^2 - 2h_m \cos \varphi_k + 1} + 1 - h_m). \quad (68)$$

When $h_m \gg 1$ one can approximate (68) as follows:

$$\nu_k^2 \approx 2J\tau_0 \sin^2 \frac{\varphi_k}{2}. \quad (69)$$

In Fig. 6 we present the results of numerical simulations performed for $N = 32, 48, 64, 128, 256$ spins. Choice of parameters: $J = 1$, $\tau_0 = 500$, $h_0 = 1, 20$. Solid lines present the results of the numerical simulations and dashed lines correspond to the asymptotic formula (33). We assume that initially the system was in the ground (ferromagnet) state. One can observe that while short wavelength excitations are essential at the critical point, at the end of evolution their contribution to the transition probability from the ground state to the first excited state is negligible. The results presented in Fig.6a show that the asymptotic for-

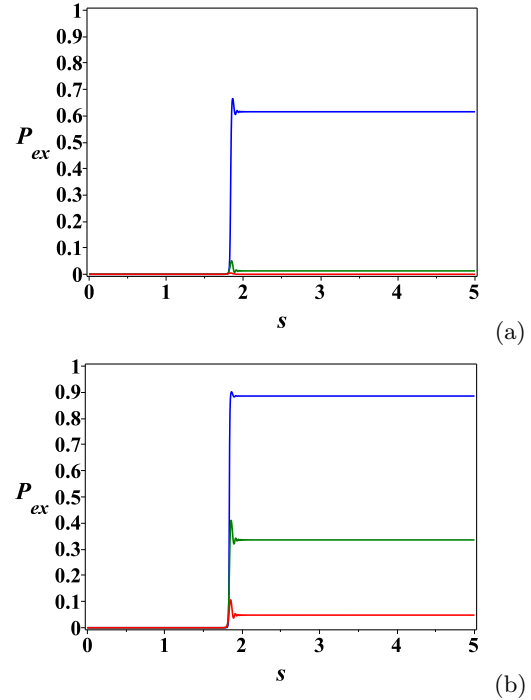


FIG. 4: (Color online) The probability P_{ex} of first excited states ($k = 1, 2, 3$) as a function of the dimensionless time s . Blue line ($k = 1$), green line ($k = 2$), red line ($k = 3$). (a) $N = 128$. (b) $N = 256$.

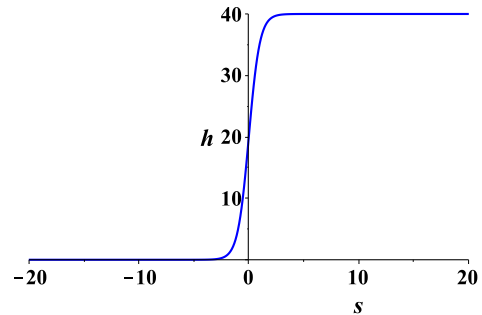


FIG. 5: (Color online) Shape of pulse, $h(s)$, as a function of dimensionless time $s = t/\tau_0$ ($h_0 = 20$).

mula (67) is in good agreement with the results of numerical simulations.

3. LZ formula and AI-approximation

In this section we compare LZ-formula and AI-approximation with the results of the numerical simulations for semi-finite pulse. We assume that initially the system was in the ground state, then the probability to stay in

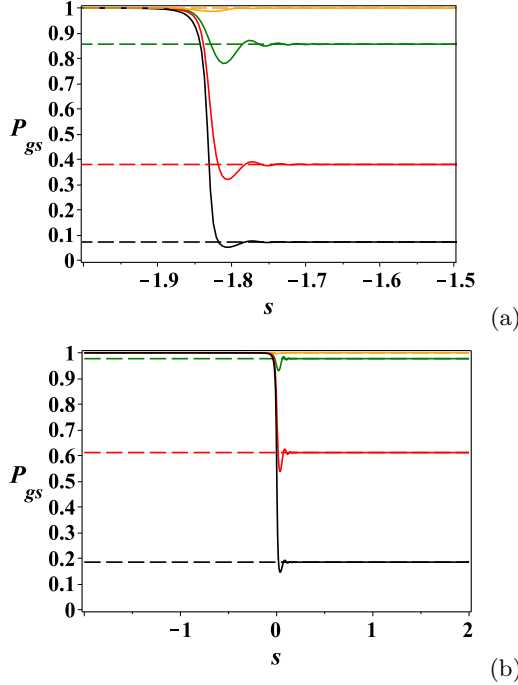


FIG. 6: (Color online) Ferromagnet \rightarrow paramagnet transition ($\tau_0 = 500$). The probability, P_{gs} , to stay in the ground state as a function of the dimensionless time $s = t/\tau_0$. Orange line ($N = 32$), green line ($N = 64$), red line ($N = 128$), black line ($N = 256$). Dashed lines correspond to the asymptotic formula (67). (a) $h_0 = 20$. (b) $h_0 = 1$.

the ground state in the end of evolution for the whole system can be written as,

$$\text{LZ} : P_{gs}^{LZ} = \prod_{k>0} (1 - e^{-x_k^2}), \quad (70)$$

$$\text{AI} : P_{gs}^{AI} = \prod_{k>0} \frac{x_k^2 + x_k \sqrt{x_k^2 + 4}}{x_k^2 + x_k \sqrt{x_k^2 + 4} + 2}, \quad (71)$$

where $x_k = \pi\omega_k^2$, the parameter of adiabaticity being $\omega_k = \sqrt{J/|\hbar_c|} \sin \varphi_k$. For the semi-finite pulse introduced in the Secs. 4.1.2. and 4.1.3, we obtain

$$\omega_k = \sqrt{\frac{\tau_0 h_0 J}{|2h_0 - 1|}} \sin \varphi_k. \quad (72)$$

In Fig. 7 we compare the predictions of LZ-formula and AI-approximation with the results of numerical simulations performed for $N = 32, 48, 64, 128, 256$ spins. Choice of parameters: $J = 1$, $\tau_0 = 500$, $h_0 = 20$. Solid lines present the results of the numerical simulations and dashed lines correspond to the asymptotic

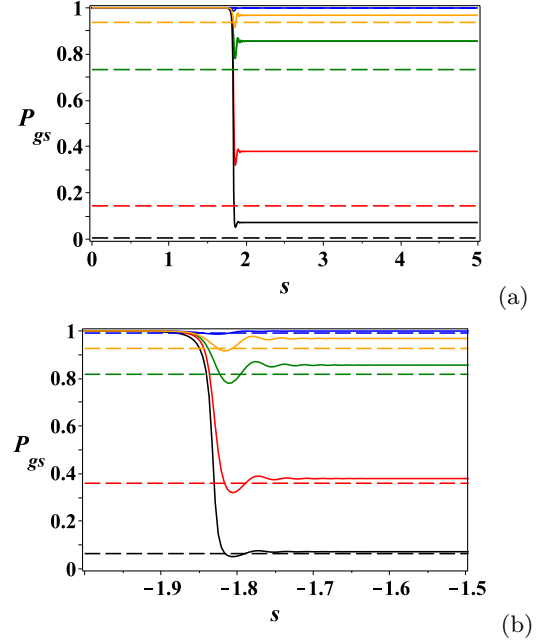


FIG. 7: (Color online) The probability, P_{gs} , to stay in the ground state as a function of the dimensionless time $s = t/\tau_0$. Blue line ($N = 32$), orange line ($N = 48$), green line ($N = 64$), red line ($N = 128$), black line ($N = 256$). (a) Paramagnet \rightarrow ferromagnet transition. Dashed lines correspond to the LZ-formula (70). (b) Ferromagnet \rightarrow paramagnet transition. Dashed lines correspond to the AI-approximation (71). Choice of parameters: $\tau_0 = 500$, $h_0 = 20$.

formulas (70) and (71). We assume that initially the system was in the ground state. In Fig. 7a the results of the paramagnet \rightarrow ferromagnet transition are presented. As expected, when the parameter of adiabaticity $\omega_k^2 \gg 1$, the LZ-formula is in good agreement with the numerical results (blue and orange curves). In Fig. 7b we compare the AI-approximation with the results of the numerical simulations for ferromagnet \rightarrow paramagnet transition. One can observe that AI-approximation is good enough for $\omega_k^2 \ll 1$ and $\omega_k^2 \gg 1$.

B. Pulse of finite length

We consider a magnetic field as a pulse of finite length with the shape determined by

$$h(\tau) = h_0 (\tanh(t/\tau_0) - \tanh(t/\tau_0 - \delta)), \quad (73)$$

the pulse length being $\Delta = \delta\tau_0$, and its height is given by $h_m = 2h_0 \tanh(\delta/2)$ (see Fig. 8).

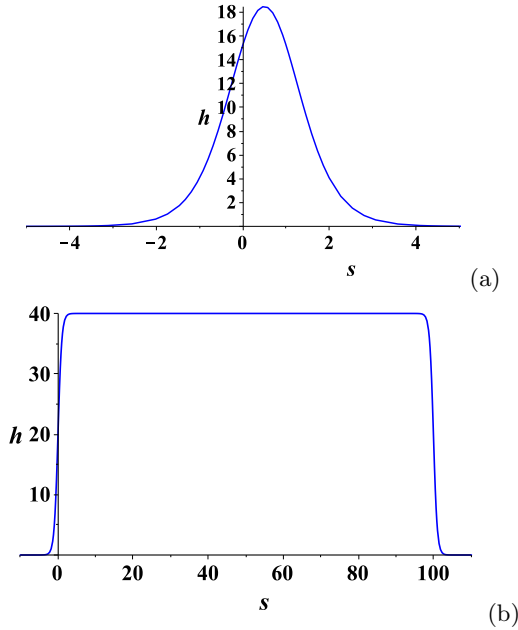


FIG. 8: (Color online) Finite pulse, $h(s)$ as a function of dimensionless time $s = t/\tau_0$ ($h_0 = 20$). (a) $\delta = 1$. (b) $\delta = 100$.

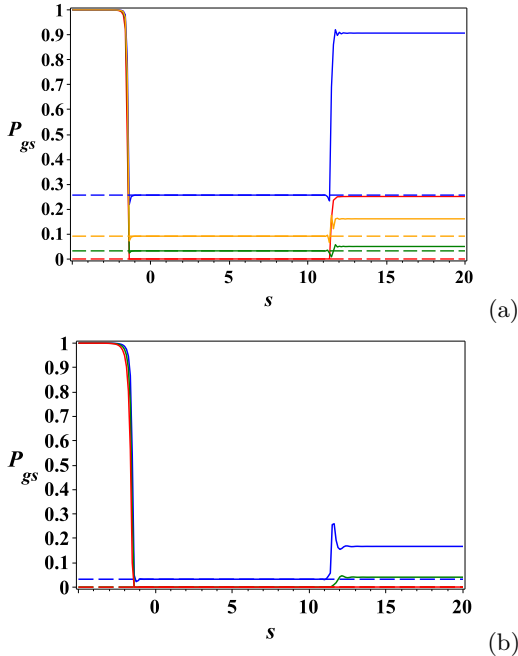


FIG. 9: (Color online) The probability, P_{gs} , to stay in the ground state as a function of the dimensionless time $s = t/\tau_0$ ($h_0 = 10$, $\delta = 10$). (a) $\tau_0 = 20$. (b) $\tau_0 = 5$. Blue line ($N = 32$), orange line ($N = 48$), green line ($N = 64$), red line ($N = 128$). Dashed lines correspond to the asymptotic formula (74).

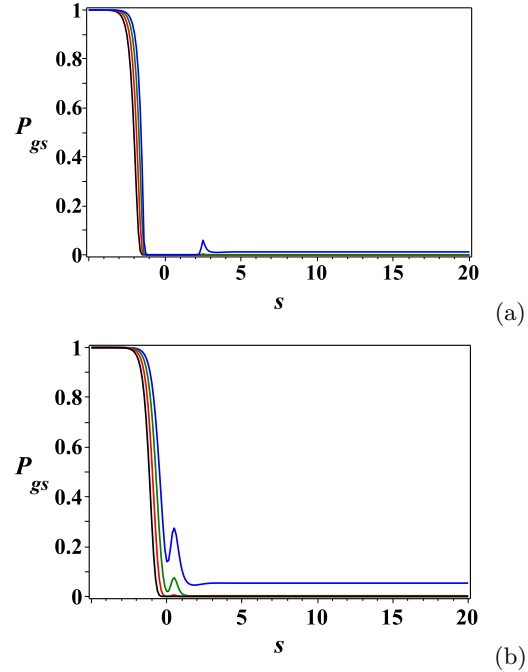


FIG. 10: (Color online) Shock wave load. The probability, P_{gs} , to stay in the ground state as a function of the dimensionless time $s = t/\tau_0$ ($h_0 = 10$, $\tau_0 = 1$). (a) $\delta = 1$. (b) $\delta = 0.1$. Blue line ($N = 32$), green line ($N = 64$), red line ($N = 128$), black line ($N = 256$).

We assume that initially the system was in the ferromagnet ground state. Near the first critical point, the quantum system becomes excited, and after crossing the critical point its state (for $h_0 \gg 1$) is determined by the number of flipped spins.

According to the KZ mechanism, the system will stay in this state up to reaching the second critical point. When the length of the pulse is relatively large, there exists the intermediate asymptotic for the probability to stay in the ground state. We find that it is given by

$$P_{gs} = \prod_k (1 - e^{-\pi \nu_k^2}), \quad (74)$$

where

$$\nu_k^2 = \tau_0 J \left(\sqrt{h_m^2 - 2h_m \cos \varphi + 1} + 1 - h_m \right). \quad (75)$$

After crossing the second critical point, the system ends in the state with the domain structure, consisting of domains with neighboring spins polarized in the same directions along the z -axis and separated by kinks (defects) in which

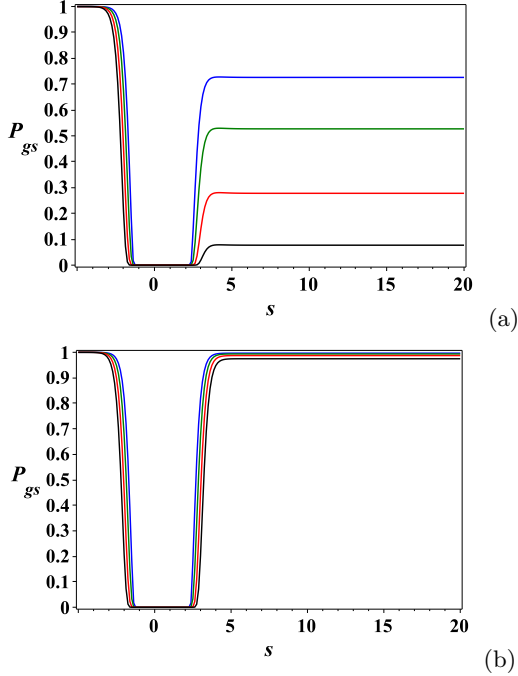


FIG. 11: (Color online) Shock wave load. The probability, P_{gs} , to stay in the ground state as a function of the dimensionless time $s = t/\tau_0$ ($h_0 = 10$, $\delta = 1$). (a) $\tau_0 = 0.01$. (b) $\tau_0 = 0.001$. Blue line ($N = 32$), green line ($N = 64$), red line ($N = 128$), black line ($N = 256$).

the polarization of spins has the opposite orientation.

In Figs. 9 - 11 we present the results of numerical simulations performed for $N = 32, 48, 64, 128, 256$ qubits. Choice of parameters: $\tau_0 = 0.001, 0.01, 1, 5, 20$, $h_0 = 10$, $\delta = 1, 10$. We assume that initially the system was in the ground (ferromagnet) state. Solid lines present the results of the numerical simulations and dashed lines correspond to the asymptotic formula (74). One can observe good agreement between the intermediate asymptotic given by Eq. (74) and the results of numerical simulations (Fig. 9).

V. CRITICAL PHENOMENA AND DEFECTS FORMATION

During its evolution the system does not stay always at the ground state at all times. At the critical point, the system becomes excited, and its final state is determined by the number of defects (kinks). Following [10], we define the operator of the number of kinks as,

$$\hat{\mathcal{N}} = \frac{1}{2} \sum_{n=1}^N (1 - \sigma_n^z \sigma_{n+1}^z) = \sum_k a_k^\dagger a_k. \quad (76)$$

Employing Eqs. (11) - (14), we obtain

$$\hat{\mathcal{N}} = \frac{N}{2} + \frac{1}{2} \sum_k \left(\cos \theta_k (c_k^\dagger c_k - c_k c_k^\dagger) + \sin \theta_k (c_k^\dagger c_{-k}^\dagger + c_{-k} c_k) \right), \quad (77)$$

The number of defects is defined by the expectation value of the operator of the number

of defects, $\mathcal{N} = \langle \hat{\mathcal{N}} \rangle$. The computation yields

$$\mathcal{N} = \frac{N}{2} + \frac{1}{2} \sum_k \left(\cos \theta_k (|v_k|^2 - |u_k|^2) + \sin \theta_k (u_k^* v_k + u_k v_k^*) \right). \quad (78)$$

In the adiabatic basis this formula takes a more simpler form,

$$\mathcal{N} = \frac{N}{2} - \frac{1}{2} \sum_k (|\alpha_k|^2 - |\beta_k|^2). \quad (79)$$

For the expectation value of the density of defects we obtain,

$$n = \frac{\mathcal{N}}{N} = 1 - \frac{1}{N} \sum_k |\alpha_k|^2. \quad (80)$$

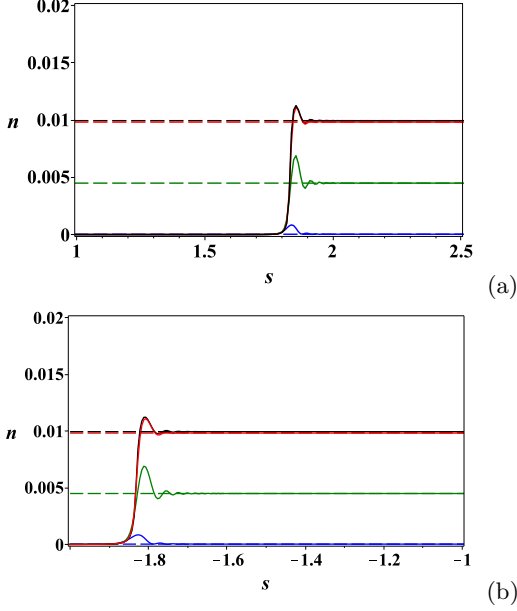


FIG. 12: (Color online) Semi-finite pulse. Density of defects vs. s ($\tau_0 = 500$, $h_0 = 20$). Blue line ($N = 32$), green line ($N = 64$), red line ($N = 128$), black line ($N = 256$). Dashed lines correspond to the asymptotic formula (81). (a) Paramagnet \rightarrow ferromagnet transition. (b) Ferromagnet \rightarrow paramagnet transition.

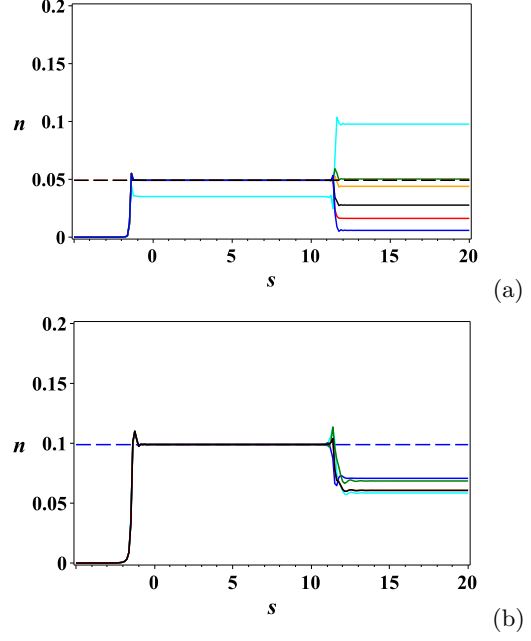


FIG. 13: (Color online) Finite pulse. Density of defects vs. s ($h_0 = 10$, $\delta = 10$). Cyan line ($N = 32$), blue line ($N = 48$), green line ($N = 64$), red line ($N = 128$), black line ($N = 256$). Dashed lines correspond to the asymptotic formula (81). (a) $\tau_0 = 20$. (b) $\tau_0 = 5$.

Denoting the probability to stay in the ground state as $P_{gs}(\varphi_k) \equiv |\alpha_k|^2$, we rewrite (80) as

$$n = 1 - \frac{1}{N} \sum_k P_{gs}(\varphi_k). \quad (81)$$

Using the approximated formula (45), we obtain

$$n \approx \frac{1}{N} \sum_k e^{4\tau_0 \Im \int_0^{z_c} \varepsilon_k(z) dz} \quad (82)$$

When $N \rightarrow \infty$, the sum in Eq. (81) can be replaced by integral,

$$n = \lim_{N \rightarrow \infty} \frac{\mathcal{N}}{N} = 1 - \frac{1}{2\pi} \int_{-\pi}^{\pi} P_{gs}(\varphi) d\varphi \quad (83)$$

Substituting $P_{gs}(\varphi)$ from Eq. (45), we find

$$n = \frac{1}{2\pi} \int_{-\pi}^{\pi} e^{-\pi\nu^2(\varphi)} d\varphi, \quad (84)$$

where

$$\nu^2(\varphi) = J\tau_0(h_m - 1 - \sqrt{h_m^2 - 2h_m \cos \varphi + 1}). \quad (85)$$

Next, using the method of steepest descent, we obtain

$$n = \frac{1}{2\pi\alpha}, \quad (86)$$

where $\alpha = 2\tau_0 J h_m / |h_m - 1|$.

As it was shown in the previous section, during the slow evolution only long wavelength modes, with the lowest $\varphi = \pi/N$, can be excited. Thus, in the adiabatic regime, $\omega_k^2 \gg 1$, we can approximate the average number of defects at the end of evolution by LZ formula,

$$n = 1 - e^{-\pi\omega^2}, \quad (87)$$

where $\omega^2 = \pi^2 \tau_0 J / N^2$ [10, 28].

In Figs. 12 -14 we compare our theoretical predictions with the results of numerical simulations performed for $N = 32, 48, 64, 128, 256$ spins. Solid lines present the results of the numerical simulations and dashed lines correspond to the asymptotic formula of Eq. (81). We assume that initially the system was in the ground state. One can observe that the results predicted by the asymptotic formula (81) are in good agreement with the numerical results.

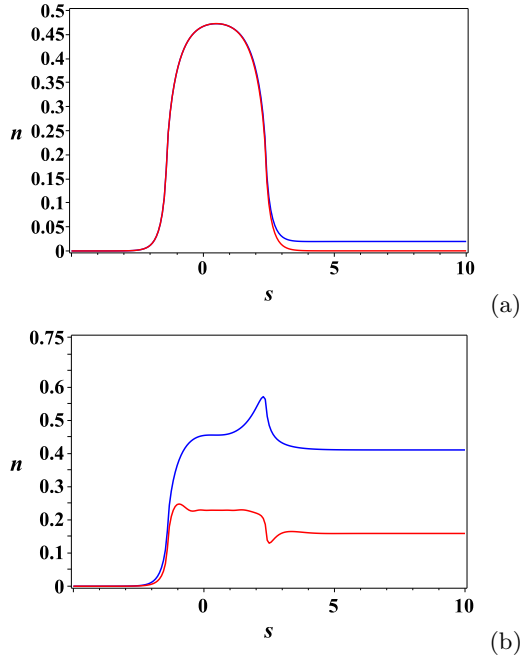


FIG. 14: (Color online) Finite pulse. Density of defects vs. dimensionless time $s = t/\tau_0$ for $N = 32, 564, 128, 256$ spins ($h_0 = 10, \delta = 1$). (a) $\tau_0 = 0.01$ (blue), $\tau_0 = 0.001$ (red). (b) $\tau_0 = 0.1$ (blue), $\tau_0 = 1$ (red).

VI. CONCLUSION

We have studied analytically and numerically the quench dynamics of the quantum Ising chain in a transverse time-dependent magnetic field. We extend the LZ-formula to non-adiabatic evolution of the quantum system. For the adiabatic evolution, our predictions coincides with the results given by the LZ-formula. Numerical simulations show good agreement between analytical and numerical results.

Under a shock-wave load the dynamics of the system is more complicated, than in the case of the semi-finite pulse. The final state of the system depends on the amplitude and pulse velocity and may results in a significant density of defects.

Acknowledgments

AIN acknowledges the support by the CONACyT.

-
- [1] S. Sachdev. *Quantum Phase Transitions*. Cambridge University Press, Cambridge, 2001.
- [2] T W B Kibble. *J. Phys. A*, **9**, 1387 (1976).
- [3] Wojciech H. Zurek. *Nature*, **317**,505 (1985).
- [4] Wojciech H. Zurek. *Phys. Rep.*, **276**, 177 (1996).
- [5] E. Lieb, T. Schultz, D. Mattis, *Ann. Phys.* **16**, 407 (1961)
- [6] S. Katsura, *Phys. Rev.* **127**, 1508 (1962)
- [7] T.D. Schultz, D.C. Mattis, E.H. Lieb, *Rev. Mod. Phys.* **36**, 856 (1964)
- [8] B.M. McCoy, *Phys. Rev.* **173**, 531 (1968)
- [9] E. Barouch, B.M. McCoy, *Phys. Rev. A* **3**, 786 (1971)
- [10] J. Dziarmaga, *Phys. Rev. Lett.* **95**, 245701 (2005).
- [11] Bogdan Damski and Wojciech H. Zurek, *Phys. Rev. A*, **73**, 063405 (2006).
- [12] Wojciech H. Zurek, Uwe Dorner, and Peter Zoller, *Phys. Rev. Lett.*, **95**,105701 (2005).
- [13] Bogdan Damski, *Phys. Rev. Lett.*, **95**, 035701 (2005).
- [14] S. Suzuki, M. Okada, in *Quantum Annealing and Related Optimization Methods, Lecture Notes in Physics*, vol. 679, ed. by A. Das, B.K. Chakrabarti (Springer, Berlin, 2005).
- [15] A. Das, B.K. Chakrabarti, *Rev. Mod. Phys.* **80**(3), 1061 (2008)
- [16] M. V. Berry, *Proc. Roy. Soc. A* **430**, 405 (1990).
- [17] A. Joye, G. Mileti, and C.-E. Pfister, *Phys. Rev. A* **44**, 4280 (1991).
- [18] H. K. A. Joye and C. E. Pfister, *Ann. Phys.* **208**, 299 (1991).
- [19] A. Kvitinsky and S. Putterman, *J. Math. Phys.* **32**, 1403 (1991).
- [20] R. Schilling, M. Vogelsberger, and D. A. Garanin, *J. Phys. A* **39**, 13727 (2006).
- [21] G. Dridi, S. Guérin, H. R. Jauslin, D. Viennot, and G. Jolicard, *Phys. Rev. A* **82**, 022109 (2010).
- [22] A. M. Dykhne, *Sov. Phys. JETP*. **14**, 941 (1962).
- [23] J. P. Davis and P. Pechukas, *J. Chem. Phys.* **64**, 3129 (1976).
- [24] J.-T. Hwang and P. Pechukas, *J. Chem. Phys.* **67**, 4640 (1977).
- [25] L. Landau, E.M. Lifshitz, *Quantum Mechanics* (Pergamon, New York, 1958)
- [26] C. Zener, *Proc. R. Soc. A* **137**, 696 (1932)
- [27] R.W. Cherng, L.S. Levitov, *Phys. Rev. A* **73**, 043614 (2006)
- [28] L. Cincio, J. Dziarmaga, M.M. Rams, W.H. Zurek, *Phys. Rev. A* **75**, 052321 (2007)